ACS OMEGA

http://pubs.acs.org/journal/acsodf

Article

Factors Affecting the Hydrophobic Property of Stearic Acid Self-Assembled on the TiO_2 Substrate

Charith Anuruddha Thennakoon,* R. B. S. Dilan Rajapakshe, Asitha Udayanga Malikaramage, and Rajapakse Mudiyanselage Gamini Rajapakse

Cite This: *ACS Omega* 2022, 7, 48184–48191

Read Online

ACCESS | Metrics & More | Article Recommendations

ABSTRACT: The self-assembled monolayer (SAM) on inorganic metal oxides is highly applicable in making different kinds of surface phenomena such as superhydrophobicity, functional group-modified surfaces, corrosion resistance, and so on. The formation of stearic acid SAMs on the TiO_2 substrate depends on a few factors, and the cleanability of the substrate surface can be considered as the critical criterion for the formation of the SAM layer. The solvent, concentration of the adsorbate, immersion time, and temperature can be identified as other factors that are crucial for growing a uniform and highly dense monolayer. SAM layers always build up spontaneously on a suitable substrate, but the growth rate and arrangement can be changed by varying the external factors. These factors highly affect the chemisorption of stearic acid molecules onto the TiO_2 substrate and building a well-ordered pattern on the surface without defects. This study mainly focuses on identifying the critical conditions of the external factors in obtaining a high-performance superhydrophobic surface. The crystal structure and surface morphologies of the substrate materials are characterized by powder X-ray diffraction and scanning electron microscopy, and the surface wettability is characterized by contact angle measurements. High superhydrophobicity is observed at the optimum conditions of the factors. Ethanol is used as the solvent; the temperature is about 40 °C; and 600 ppm of stearic acid is the critical concentration in obtaining a superhydrophobic surface with 100 min of immersion time, while the contact angle is 151.38°. Simultaneously, if the concentration is 1000 ppm and the immersion time is 120 min, the surface shows high superhydrophobicity with a contact angle of 162.06°. These critical conditions are found to be adequate for building well-ordered stearic acid SAMs on the TiO_2 substrate.

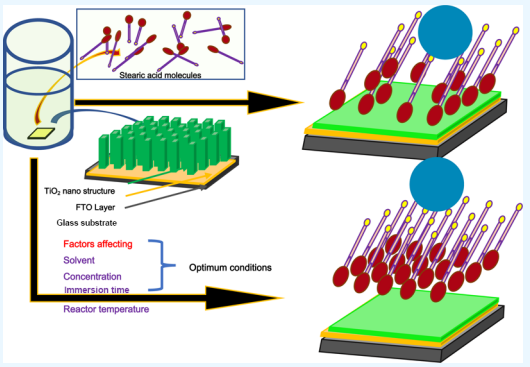

1. INTRODUCTION

The self-assembled monolayer (SAM) is a two-dimensional molecular arrangement that is spontaneously arranged in an ordered homogeneous pattern by the spontaneous adsorption of molecules from the gas or liquid phase onto surfaces. This SAM arrangement is formed spontaneously by the chemisorption process of the organic molecule on a given surface and organized into a more or less ordered zone.[1] The building blocks of the SAM are organized by utilizing weak interactions, which are the van der Waals bond and hydrogen bond. The arrangement of such fundamental building blocks can be spontaneously formed from a solution in which intermolecular forces play a major role and are adsorbed on solid surfaces. Both head and terminal end groups are present in the molecule that is used for the construction of the building blocks of SAM.[2−4] These amphiphilic molecules can provide highly ordered monolayers with nearly defect-free coverage under appropriate conditions, while the head group can provide a strong binding with the surface. Gold[5,6] on silver, carboxylic acids on metal oxides,[7] alkyl phosphonic acids on mica,[8,9] and alkyl silane on a SiO_2 surface[10] are a few good examples of the building blocks of SAM. The chain length of the amphiphilic adsorbate is impacted by the growth of a well-arranged SAM layer.[11] Various experimental parameters influence the strong packing arrangement of SAM, including the solvent, temperature, immersion time, and concentration of the adsorbate. When optimizing the abovementioned parameters, a good array of the surface can be observed.[12] SAMs are well suited for studies in the nanoscience and nanotechnological areas as they are easy to be constructed as different kinds of surfaces such as thin films, nanoparticles, nanowires, nanocages in colloids, and so on. Few common organic amphiphilic materials are popular in behaving as adsorbates due to their head and tail groups.

Received: September 26, 2022
Accepted: November 28, 2022
Published: December 13, 2022

Alkane with the carboxylic acid head group, organo-thiol, organo-silane, and so on,[13] are a few such examples. The uniform high coverage and stability make SAMs ideal for many technological applications, such as lubrication of the underlying substrate surface, corrosion inhibition by passivation of the surface, surface patterning as photoresists, diffusion barriers, and prevention of nonspecific adsorption and befouling.[14]

There are many kinds of surfaces that have been modified by the impact of self-assembly adsorption. Organic amphiphilic molecules can produce a well-ordered arrangement on a substrate which is a simple immersion into a solution. The functional group of the amphiphilic organic molecules is called a head group, which is coordinated with the substrate. These head groups can be adsorbed chemically with −OH groups on the substrate. If the substrate has more hydroxyl groups, then the self-assembling density is higher than the normal surface.[15,16]

Here, stearic acid adsorption on the TiO_2 surface is studied with different external factors, which are the solvent for stearic acid (adsorbate), immersion time, concentration of the adsorbate, and temperature of the system. In this study, the adsorption efficiency and performance are analyzed by the surface wettability of the substrate in terms of contact angle measurement. The TiO_2 nanolayer is grown on the fluorine-doped tin oxide (FTO) substrate by the hydrothermal synthesis method in which a similar and uniform surface morphology is obtained. Acetone, ethanol, methanol, and ethyl acetate are used as solvents to dissolve the stearic acid, and they are selected according to their solubility. As a first step, a suitable solvent is identified for modifying the super-hydrophobic surface; second, the optimum and minimum immersion time with the concentration of stearic acid for building up a well-ordered SAM layer are identified. Then, surface wettabilities are analyzed under different conditions of the abovementioned parameters. Finally, the behavior of the SAM mechanism is studied by changing the system temperature.

2. EXPERIMENTAL SECTION

2.1. Chemicals and Materials. Titanium(iv) isopropoxide (TTIP), stearic acid, ethanol (absolute and pure), glacial acetic acid, FTO glass plates, a 100 mL Teflon vessel autoclave, ethyl acetate, methanol, and acetone were used in the study. All chemicals were purchased from Sigma-Aldrich.

2.2. Methodology. *2.2.1. Growing a TiO_2-Nanostructured Uniform Layer on FTO Glass Plates.* First, 5.0 mL of hydrochloric acid (HCl) and 5.0 mL of distilled water were added to a 50.0 mL beaker and stirred well at room temperature. After 10 min, 400 μL of TTIP was added to the beaker slowly and stirred continuously for another 30 min at room temperature. Simultaneously, 1.0 × 1.0 cm FTO glass plates were cleaned by ultra-sonication with detergents for 15 min. The cleaned glass plates were dried and kept in a Teflon vessel autoclave, keeping the FTO-coated side up. Then, 10.0 mL of TiO_2 precursor solution was put onto glass plates kept in the Teflon vessel autoclave, then it was sealed tightly, and kept in an oven for 4 h at 150 °C. After that, the autoclave was kept in the oven to naturally cool down. Finally, the TiO_2-coated glass plates were sintered by a muffle furnace at 450 °C for 1 h.

2.2.2. Interpretation of Self-Assembly with Different Solvents (Methanol, Ethanol, Ethyl Acetate, and Acetone), Concentrations, Immersion Times, and Temperatures. First, 1000 ppm of stearic acid solution was prepared in 50 mL of each (methanol, ethanol, ethyl acetate, and acetone) different solvent. Then, four TiO_2-deposited glass substrates were dipped in each solvent for 2 h at room temperature. As a next step, seven stearic acid samples were made with different concentrations, 200, 400, 600, 800, and 1000 ppm, by dissolving pure ethanol in Petri dishes. Six Petri dishes were prepared in each concentration to identify their immersion times which are 20, 40, 60, 80, 100, and 120 min. All the reaction vessels were kept at room temperature, and after the immersion, each glass substrate was taken out of the solution and washed with hot ethanol (around 40 °C) twice, and the substrates were dried in an oven at 80 °C for 30 min. Finally, 1000 ppm of stearic acid was dissolved in 50 ml of ethanol, and seven samples were made with the same chemical ratios. There were seven TiO_2 nanolayer-deposited glass substrates dipped in stearic acid solution, and all the samples were kept at different temperatures which, were 20, 25, 30, 35, 40, 45, and 50 °C. After the immersion, all the substrates were taken off the dishes and washed with ethanol to remove unassembled stearic acid molecules. Finally, all the substrates were dried at 80 °C for 30 min.

3. RESULTS AND DISCUSSION

Four different solvents, five different concentrations of the adsorbate, six different time durations, and seven different temperatures are the considered parameters of the factors. A number of contact angle measurements are done by changing their external parameters (Figure 1).

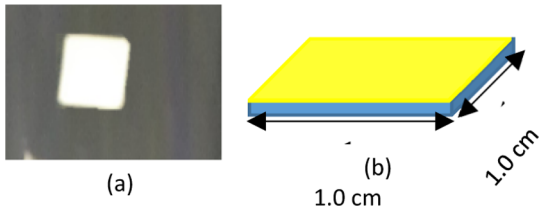

Figure 1. TiO_2 nanolayer-deposited FTO glass substrate: (a) optical image of the substrate and (b) sketch of the substrate.

3.1. X-ray Diffraction Analysis of the TiO_2-Deposited FTO Substrate. X-ray diffraction (XRD) analysis of the TiO_2 thin layer on the glass substrate is shown in Figure 2. The diffraction pattern shows a good arrangement of the TiO_2 structure, which is in the metastable anatase form and brookite form, as well as the little arrangement of the stable rutile form.

TiO_2 is in the metastable anatase form at low temperatures, and here some rutile peaks can be seen because of sintering.[17−19] However, the main diffraction peak at the position of Bragg's angle of 25.2° (101) is observed in the anatase form of TiO_2 (Figure 2). Moreover, other peaks which are relevant for the TiO_2 anatase form are located in the positions of Bragg's angles of 37, 48, 53, and 62°, corresponding to the planes of (103), (004), (200), and (301), respectively. The remaining peaks are observed due to the rutile form of TiO_2, as well as the brookite form.[20−23] The rutile form of TiO_2 is located at the position of Bragg's angle of 27.45°, corresponding to the plane of (110).[24−26] However, other peaks of the rutile form could not be observed since such crystal planes are not formed by the applied conditions. Moreover, Bragg's angle corresponds to the brookite form,

https://doi.org/10.1021/acsomega.2c06217
ACS Omega 2022, 7, 48184−48191

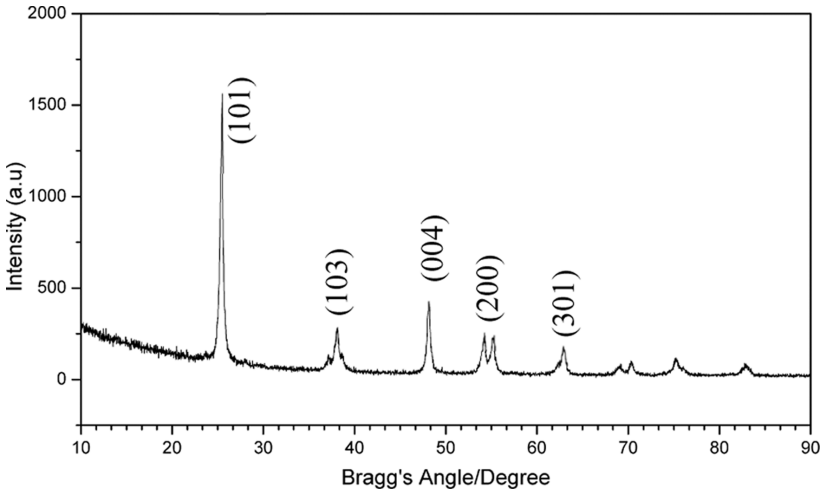

Figure 2. XRD pattern of TiO_2 grown on the FTO glass plate.

where a peak is located at 32.81° corresponding to the (020) plane.[27−29] Here, there are no other peaks that correspond to the brookite form. Both the rutile and brookite forms have only one Brag's diffraction position, which is described as a monoplane for the brookite and rutile forms.

3.2. Morphological Analysis of the TiO_2 Nanolayer-Deposited Substrate. SEM images of randomly selected two glass substrates are shown in Figure 3. Figure 3a,b shows the same glass substrate at different magnifications. Figure 3c,d shows the same substrate with different magnifications. When considering all the SEM images, surface morphology can be identified clearly, showing rod-like structures.

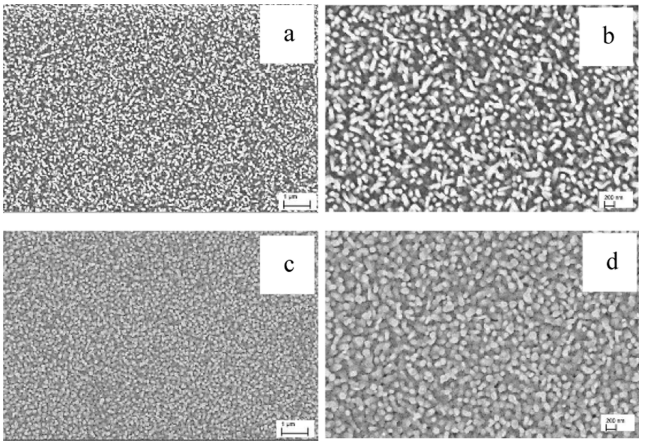

Figure 3. SEM images of randomly selected two glass plates with the grown TiO_2 nanolayer: (a, b) same glass substrate with different magnificationsand (c, d) another substrate with different magnifications.

A TiO_2 nanolayer has been grown in a highly uniform, dense layer with almost similar particles with a diameter of around 50 nm. FTO is the best substrate to grow TiO_2 rod-like structures with strong adhesion. A TiO_2 precursor solution is used for growing the TiO_2 on FTO glass plates, during which the precursor solution is converted into TiO_2 particles inside the autoclave, and then, TiO_2 nanostructured layer is grown on the FTO substrate.

3.3. Growth of SAMs on the TiO_2 Substrate with Different Solvents. Solvents are affected in the making of self-assembling monolayers on a given substrate. Stearic acid dissolved in different solvents gives different SAM layers on the TiO_2 substrate, which can be distinguished by their contact angles.

Understanding of the stearic acid self-assembled onto the TiO_2 substrate can be explained by their protic and aprotic solvent behaviors (Table 1). When ethanol and methanol are used as the solvent, it shows higher water contact angles (Figure 4a,b) than the ethyl acetate and acetone complex (Figure 4c,d). The results mean that the surface structure and the nondefective surface morphology are strongly influenced by the solvents. Such a packing arrangement of the stearic acid on the TiO_2 substrate should be well-ordered due to the results of contact angle measurements of each solvent.[32,33]

Dielectric property is another important factor in the choice of solvent for making highly uniform and dense monolayers on a given substrate.[31] When considering both the protic solvents, ethanol shows a lower dielectric constant than methanol, which are, respectively, 24.55 and 32.70. Ethanol shows the highest contact angle of 151.35°, and methanol shows a contact angle of around 150.04° (Table 1) due to the formation of the SAM layer. Parallelly, the aprotic solvents also behave according to the theory of the dielectric constant of ethyl acetate and acetone. Both the solvents are polar and

Table 1. Solubility, Dielectric Constant, Protic/Aprotic Behavior of Stearic Acid, and Contact Angle of the Substrate in Different Solvents[30−32]

solvent	solubility/mol dm^{-3}	contact angle/degree	dielectric constant	protic/aprotic
ethanol	10.5×10^3	151.35	24.55	protic
methanol	2.7×10^3	150.04	32.70	protic
ethyl acetate	13.9×10^3	124.50	6.02	aprotic
acetone	9.1×10^3	101.63	20.70	aprotic

https://doi.org/10.1021/acsomega.2c06217
ACS Omega 2022, 7, 48184−48191

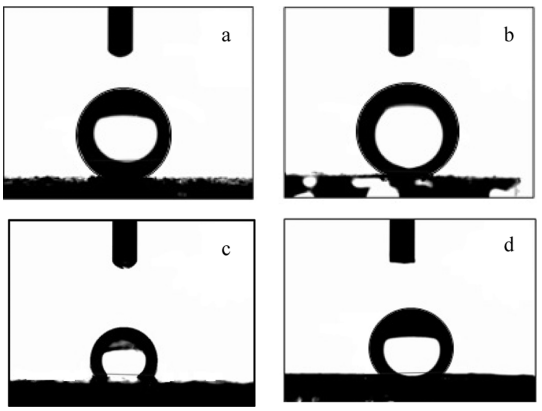

Figure 4. Measurements of contact angle with different solvents: (a) ethanol, (b) methanol, (c) acetone, and (d) ethyl acetate.

aprotic, and their dielectric constants are respectively 6.02 and 20.70 (Table 1). The contact angle measurements of the stearic acid SAM layer under the abovementioned two solvents are 124.50 and 101.63°, which proves the dielectric constants are in the descending order of the well-ordered SAM layer. Generally, defects are created on the SAM-modified substrate with the potential of the dielectric constant, which shows the low contact angle measurements due to the ununiform and low-density packing arrangement of stearic acid on the TiO_2.[34] Furthermore, the stearic acid solubilities of each solvent is the possible cause for the higher contact angle measurement since the solute concentration, and the solvents are good carriers for the interaction between solute and the substrate.

However, a total understanding of how solvents affect a well-ordered SAM layer is very complicated due to other solvent properties, including polarity, molecular diameter, and viscosity, as these may affect the chemisorption of stearic acid molecules onto the TiO_2 surface while building up the SAM layer.

3.4. Growth of SAMs with Different Immersion Times and Concentrations of Stearic Acid in Ethanol. The concentration of stearic acid (adsorbate) and the immersion time are the other two important factors in making a well-ordered hierarchical SAM layer on the TiO_2 substrate. When considering the concentration of the stearic acid, which is highly effective in building up the SAM layer as it depends on the amount of reactive molecules and the mobility. However, the immersion time is also affected by the building up of a well-

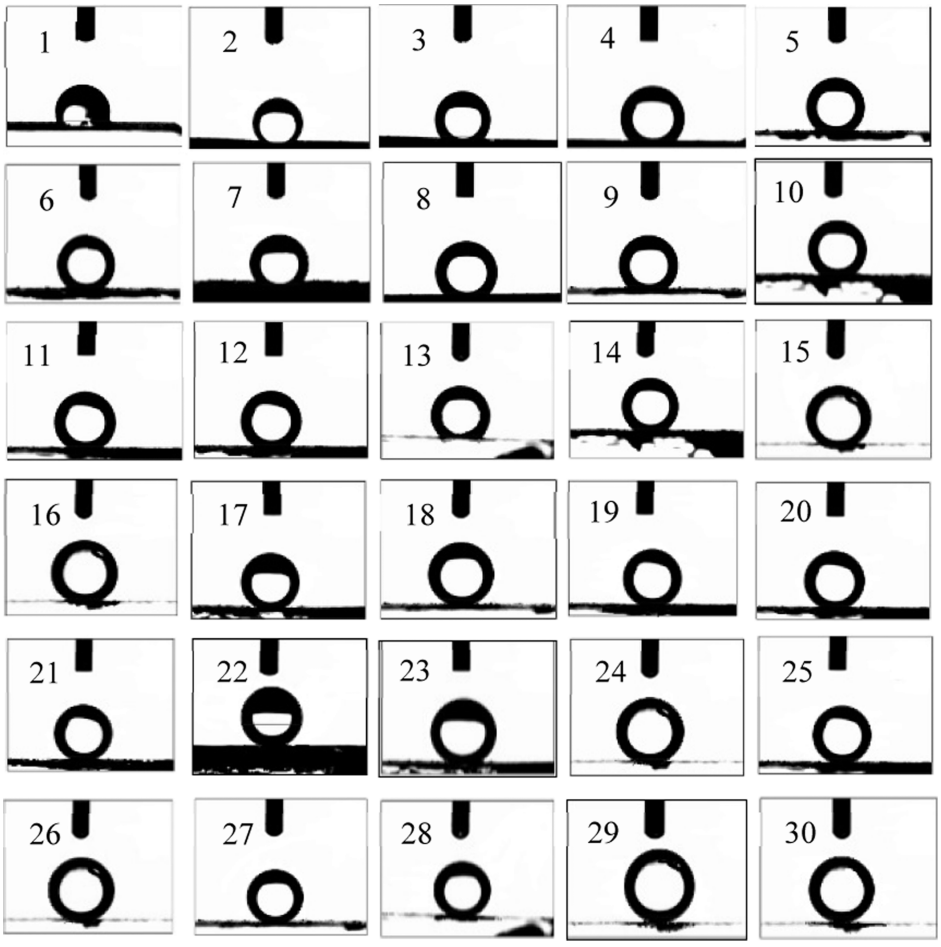

Figure 5. Contact angle measurements: (1−-5) at concentrations of 200, 400, 600, 800, and 1000 ppm, respectively, with an immersion time of 20 min, (6−10) at concentrations of 200, 400, 600, 800, and 1000 ppm, respectively, with an immersion time of 40 min, (11−15) at concentrations of 200 ppm, 400 ppm, 600 ppm, 800 ppm, and 1000 ppm, respectively, with an immersion time of 60 min, (16−20) at concentrations of 200, 400, 600, 800, and 1000 ppm, respectively, with an immersion time of 80 min, (21−25) at concentrations of 200, 400, 600, 800, and 1000 ppm, respectively, with an immersion time of 100 min, and (26−30) at concentrations of 200, 400, 600, 800, and 1000 ppm, respectively, with an immersion time of 120 min.

https://doi.org/10.1021/acsomega.2c06217
ACS Omega 2022, 7, 48184−48191

arranged SAM layer. A well-ordered SAM layer can be observed at the optimum values of concentration and immersion time. In a high-concentration stearic acid solution, the SAM layer grows up with a shorter immersion time, and in a low-concentration stearic acid solution, it takes a relatively longer immersion time. However, the optimum conditions of both the concentration and immersion time are identified by analyzing their contact angle measurements. Contact angles of all the substrates are presented in Figure 5, and the surfaces' wettability varies with the immersion time and their concentrations. In Figure 5, horizontal lines show contact angles at different concentrations of stearic acid with a constant time, and vertical directions show their contact angles for different immersion times with a constant concentration of stearic acid. All the contact angles are shown in Table 2 with their corresponding concentrations and immersion times.

Table 2. Contact Angle Measurements with Different Concentrations of Stearic Acid and Immersion Times

	concentration of stearic acid in ethanol/ppm				
time/minutes	200 (deg)	400 (deg)	600 (deg)	800 (deg)	1000 (deg)
20	108.32	121.66	133.82	144.22	151.00
40	120.02	128.46	142.63	147.36	155.72
60	127.10	135.48	147.46	150.22	158.26
80	132.42	140.82	149.00	152.04	160.04
100	136.00	143.34	151.38	153.86	161.54
120	137.02	144.06	152.22	154.04	162.06

Basically, both factors are more effective in building up a well-ordered SAM layer on the TiO_2 surface (Figure 6). After 60 min of immersion for all the concentrations of the adsorbate, the increment of the contact angles is relatively low. In the initial stage, which is before 60 min of immersion time, it has a higher mobility of adsorbate, and there are many −OH groups available in the oxide material for assembling the adsorbate. Due to that reason, high contact angles are shown during the immersion time.

All the substrates with various concentrations of stearic acid (200, 400, 600, 800, and 1000 ppm) and 60 min of immersion time showed high contact angles of 127.10, 135.48, 147.46, 150.22, and 158.26°, respectively (Table 2). According to Figure 6, the increment in the contact angles is reduced after 60 min of immersion time due to the low concentration of the adsorbate in the medium, the low reactive sites of the particles (−OH groups), and steric hindrance caused by the assembled adsorbate molecules. When considering the variation of the contact angles with the immersion time, contact angles are increased after the time of 60 min, but the rates of increment are very low. When considering the 200 ppm series, initially, they show very low contact angles that are about 108.32°, and after 120 min, they become 139.02°. The same performance can be obtained in the stearic acid, in which the concentration is 600 ppm with a low immersion time of around 20 min. In fact, adsorbate concentrations of 200 and 400 ppm do not exceed the superhydrophobic range even after 120 min. The growth rate is very low and almost zero after 100 min, where the contact angles can be observed around 136.00 and 137.02° at concentrations of 200 ppm and 400 ppm, respectively. However, when considering the adsorbate concentrations of 600, 800, and 1000 ppm, those have passed the superhydrophobic range (contact angle 150°) with corresponding immersion times. In a solution of 600 ppm concentration, the substrate shows superhydrophobicity when it is immersed for 110 min in the adsorbate. Moreover, when the substrate is at 800 ppm adsorbate, it shows superhydrophobicity after 60 min of immersion time. Also, when the substrate is in a 1000 ppm solution of the adsorbate, the superhydrophobicity is shown after 20 min.

According to the available results in Figures 6 and 7, superhydrophobicity is observed at concentrations greater than 600 ppm, where the immersion time is 100 min. If the concentration is higher than 600 ppm, it is giving the same or higher performance of superhydrophobicity even with a low immersion time. Finally, the optimum concentration can be described as being greater than 600 ppm, and the immersion time should generally be in the range of 20 to 100 min and the time durations should be relevant to the concentrations.

3.5. Growth of SAMs at Different Temperatures. The temperature of the reactor medium can be described as

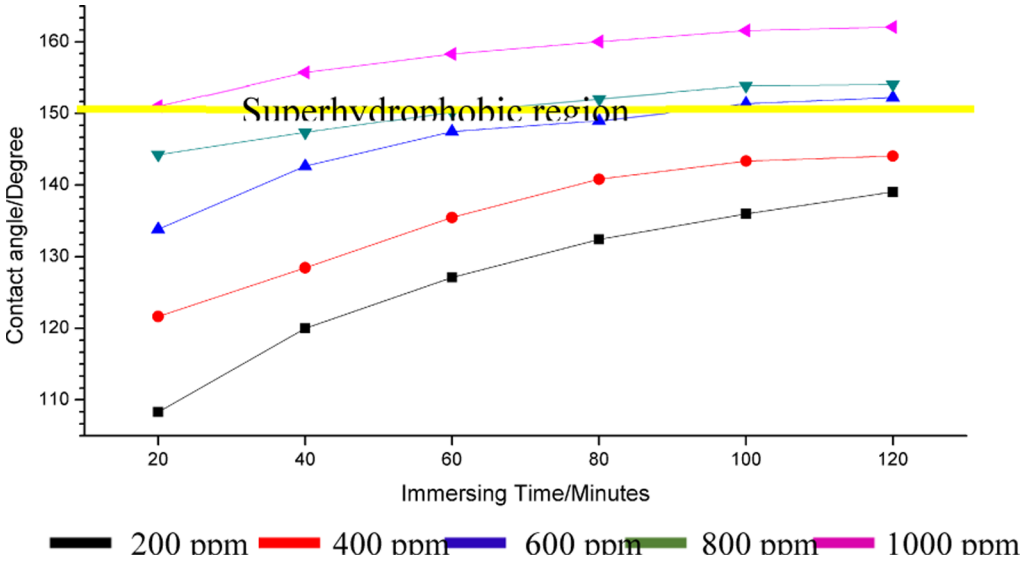

Figure 6. Graph of contact angle variation with the constant concentration of stearic acid and immersion time.

https://doi.org/10.1021/acsomega.2c06217
ACS Omega 2022, 7, 48184−48191

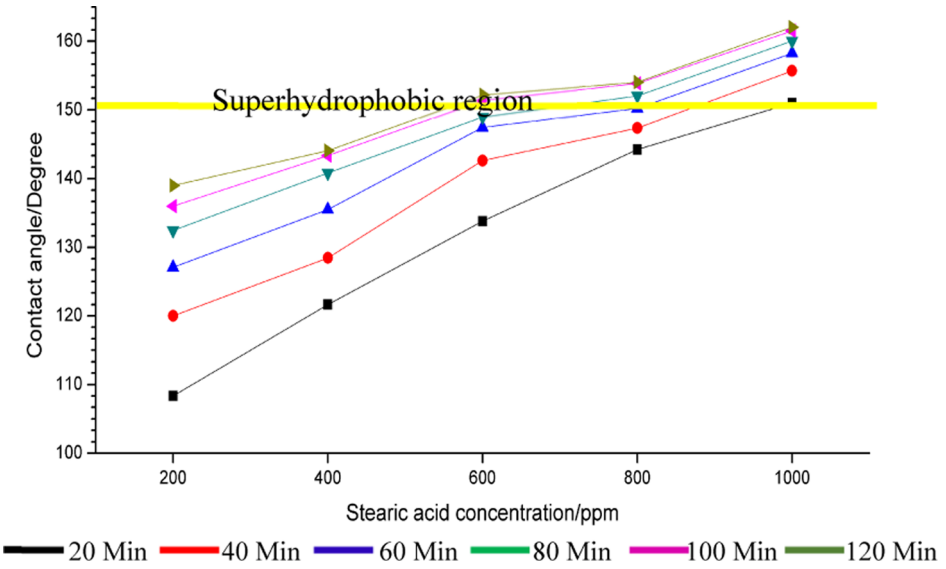

Figure 7. Contact angle variation with a constant immersion time and different concentrations of stearic acid.

another important factor in building up the SAM layer on a given substrate. Generally, SAM layers are modified at room temperature, which is not a constant as it varies by location and season. However, finding an optimum temperature is important for building up a well-ordered SAM layer on a given substrate. Generally, when the SAM temperature is above 25 °C, this can improve their kinetics of formation with a smaller number of defects and help in making well-arranged surfaces.

The stearic acid SAM layer on the TiO_2 substrate is described using the contact angle, and the contact angle variations can be observed in Figure 8, and the measurements are given in Table 3.

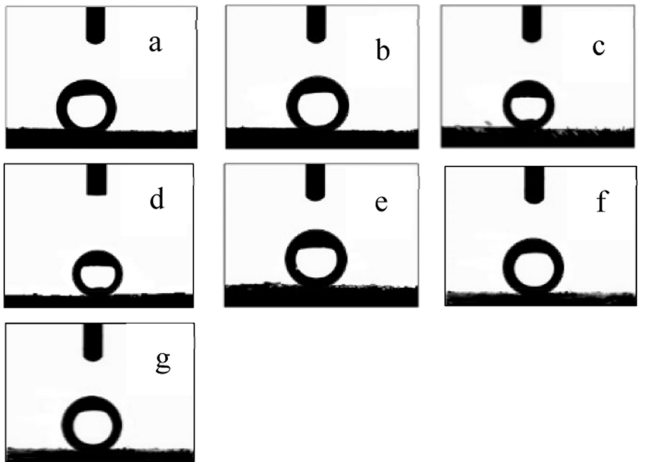

Figure 8. Contact angle measurements at different temperatures: (a) 20 °C, (b) 25 °C, (c) 30, (d) 35 °C, (e)40 °C, (f) 45 °C, and (g) 50 °C.

Generally, a temperature that is higher than the room temperature is particularly used as it is effective in performance. However, when increasing the temperature above 40 °C, some defects can be introduced in the SAM layer due to the desorption process (Figure 9). Up to 40 °C of elevated temperature, the SAM layer is building up with a good arrangement of the surface without any defects, and it is clarified by the contact angles.

Finally, the temperature of the reactor is not of high importance as it does not improve the performance of the substrate much. However, 40 °C is the effective temperature of the reactor to make the highly ordered stearic acid SAM layer on the TiO_2 substrate.

4. CONCLUSIONS

When considering all the factors for building up stearic acid SAM layers on the TiO_2 substrate, ethanol can be identified as the best solvent for obtaining good superhydrophobicity. The concentration of the stearic acid and the immersion time are more important for the SAM layer, but the time and concentrations can be selected according to the process requirements. Moreover, the high-concentration adsorbate requiers a low immersion time, whereas the low-concentration adsorbate requires a high immersion time in obtaining the same superhydrophobic performance. However, the concentration should be above the limit of the critical adsorbate concentration, which is 600 ppm. TiO_2 can disperse well in the medium of ethanol, and the stearic acid solubility is high in the medium. Concentration and immersion time are analyzed together, and there is a correlation between those two. 600 ppm of stearic acid is the optimum critical concentration for making a well-arranged SAM layer on the TiO_2 surface, and the relevant immersion time is 100 min, while the contact angle is about 151.38°. If the concentration of the adsorbate is

Table 3. Contact Angle Measurements at Different Temperatures

	temperature/°C						
	20	25	30	35	40	45	50
contact angles/degree	144.88	153.32	153.82	154.02	154.36	153.12	149.84

https://doi.org/10.1021/acsomega.2c06217
ACS Omega 2022, 7, 48184−48191

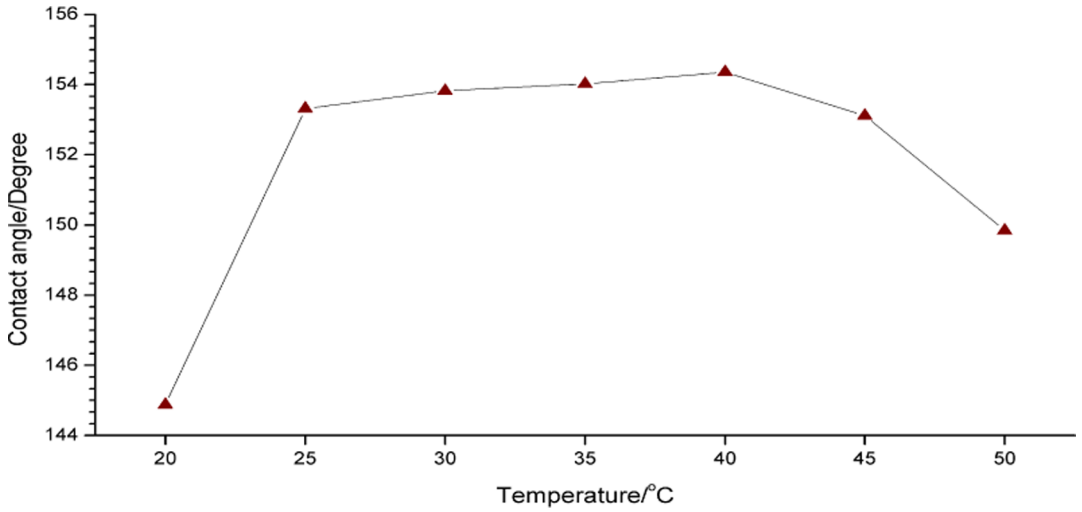

Figure 9. Contact angle variation with different temperatures of the reaction vessel.

1000 ppm, the immersion time is decreased to 20 min with a contact angle of 151.00°. If the concentration is 1000 ppm and the immersion time is 120 min, the surface is performing high superhydrophobicity with a contact angle of 162.06°. The relationship between the concentration and the immersion time is an inversely proportional correlation. As the temperature of the reactor is increased up to 40 °C, the contact angle of the substrate is also increased, and then the contact angle is decreased after 40 °C of reactor temperature.

AUTHOR INFORMATION

Corresponding Author

Charith Anuruddha Thennakoon − *Department of Chemistry, Faculty of Science, University of Peradeniya, Peradeniya 20400, Sri Lanka; Postgraduate Institute of Science, University of Peradeniya, Peradeniya 20400, Sri Lanka;* orcid.org/0000-0002-7889-3115; Email: charith.pdn@gmail.com

Authors

R. B. S. Dilan Rajapakshe − *Department of Chemistry, Faculty of Science, University of Peradeniya, Peradeniya 20400, Sri Lanka; Postgraduate Institute of Science, University of Peradeniya, Peradeniya 20400, Sri Lanka*

Asitha Udayanga Malikaramage − *Department of Chemistry, Faculty of Science, University of Peradeniya, Peradeniya 20400, Sri Lanka; Postgraduate Institute of Science, University of Peradeniya, Peradeniya 20400, Sri Lanka*

Rajapakse Mudiyanselage Gamini Rajapakse − *Department of Chemistry, Faculty of Science, University of Peradeniya, Peradeniya 20400, Sri Lanka; Postgraduate Institute of Science, University of Peradeniya, Peradeniya 20400, Sri Lanka;* orcid.org/0000-0003-3943-5362

Complete contact information is available at: https://pubs.acs.org/10.1021/acsomega.2c06217

Notes

The authors declare no competing financial interest.

ACKNOWLEDGMENTS

The authors gratefully acknowledge the National Science Foundation, Sri Lanka (grant TG/2014/Tech-D/04) and the Faculty of Science, University of Peradeniya, Sri Lanka, for financial support.

REFERENCES

(1) Jadhav, S. A. Self-assembled Monolayers (SAMs) of Carboxylic Acids: An overview. *Cent. Eur. J. Chem.* **2011**, *9*, 369−378.

(2) Markovich, I.; Mandler, D. Disorganised Self-assembled Monolayers (SAMs): the Incorporation of Amphiphilic Molecules. *Analyst* **2001**, *126*, 1850−1856.

(3) Kumara, M. T.; Tripp, B. C.; Muralidharan, S. Layer-by-Layer Assembly of Bioengineered Flagella Protein Nanotubes. *Biomacromolecules* **2007**, *8*, 3718−3722.

(4) Lim, M. S.; Feng, K.; Chen, X.; Wu, N.; Raman, A.; Nightingale, J.; Gawalt, E. S.; Korakakis, D.; Hornak, L. A.; Timperman, A. T. Adsorption and Desorption of Stearic Acid Self-Assembled Monolayers on Aluminum Oxide. *Langmuir* **2007**, *23*, 2444−2452.

(5) Kim, H. I.; Koini, T.; Lee, T. R.; Perry, S. S. Molecular Contributions to the Frictional Properties of Fluorinated Self-Assembled Monolayers. *Tribol. Lett.* **1998**, *4*, 137−140.

(6) Shon, Y.; Lee, T. R. Desorption and Exchange of Self-Assembled Monolayers (SAMs) on Gold Generated from Chelating Alkanedithiols. *J. Phys. Chem. B* **2000**, *104*, 8192−8200.

(7) Rieley, H.; Kendall, G. K.; Jones, R. G.; Woodruff, D. P. X-ray Studies of Self-Assembled Monolayers on Coinage Metals. 2. Surface Adsorption Structures in 1-Octanethiol on Cu(111) and Ag(111) and Their Determination by the Normal Incidence X-ray Standing Wave Technique. *Langmuir* **1999**, *15*, 8856−8866.

(8) Doudevski, I.; Schwartz, D. K. Mechanisms of Self-Assembled Monolayer Desorption Determined Using in Situ Atomic Force Microscopy. *Langmuir* **2000**, *16*, 9381−9384.

(9) Nie, H.; Miller, D. J.; Francis, J. T.; Walzak, M. J.; McIntyre, N. S. Robust Self-Assembled Octadecylphosphonic Acid Monolayers on a Mica Substrate. *Langmuir* **2005**, *21*, 2773−2778.

(10) Roscioni, O. M.; Muccioli, L.; Mityashin, A.; Cornil, J.; Zannoni, C. Structural Characterization of Alkylsilane and Fluoroalkylsilane Self-Assembled Monolayers on SiO2 by Molecular Dynamics Simulations. *J. Phys. Chem. C* **2016**, *120*, 14652−14662.

(11) Lee, S.; Shon, Y.; Colorado, R.; Guenard, R. L.; Lee, T. R.; Perry, S. S. The Influence of Packing Densities and Surface Order on the Frictional Properties of Alkanethiol Self-Assembled Monolayers (SAMs) on Gold: A Comparison of SAMs Derived from Normal and Spiroalkanedithiols. *Langmiur* **2000**, *16*, 2220−2224.

(12) Luedtke, W. D.; Landman, U. Structure and Thermodynamics of Self-Assembled Monolayers on Gold Nanocrystallites. *J. Phys. Chem. B* **1998**, *102*, 6566−6572.

(13) Pertays, K. M.; Thompson, G. E.; Alexander, M. R. Self-assembly of Stearic Acid on Aluminium: The importance of oxide surface chemistry. *Surf. Interface Anal.* **2004**, *36*, 1361−1366.
(14) Chen, J.; Chang, B.; Oyola-Reynoso, S.; Wang, Z.; Thuo, M. Quantifying Gauche Defects and Phase Evolution in Self-Assembled Monolayers through Sessile Drops. *ACS Omega* **2017**, *2*, 2072−2084.
(15) Thennakoon, C. A.; Rajapakshe, R. B. S. D.; Rajapakse, R. M. G.; Rajapakse, R. G. S. C. Anti-stain and durable superhydrophobic/antistatic dual functionality surface for fabric materials based on F-ZnO/TiO2 composite. *J. Sol-Gel Sci. Technol.* **2022**, *101*, 529−538.
(16) Paz, Y. Self-Assembled Monolayers and Titanium Dioxide: from Surface Patterning to Potential Applications. *Beilstein J. Nanotechnol.* **2011**, *2*, 845−861.
(17) Helmy, R.; Fadeev, A. Y. Self-Assembled Monolayers Supported on TiO2: Comparison of C18H37SiX3 (X = H, Cl, OCH3), C18H37Si(CH3)2Cl, and C18H37PO(OH)2. *Langmuir* **2002**, *18*, 8924−8928.
(18) Hosseini, S. N.; Chen, X.; Baesjou, P. J.; Imhof, A.; van Blaaderen, A. Synthesis and Characterization of Anatase TiO_2 Nanorods: Insights from Nanorods' Formation and Self-Assembly. *Appl. Sci.* **2022**, *12*, 1614.
(19) Wu, C. U.; Tu, K. J.; Deng, J. P.; Lo, Y. S.; Wu, C. H. Markedly Enhanced Surface Hydroxyl Groups of TiO2 Nanoparticles with Superior Water-Dispersibility for Photocatalysis. *Materials* **2017**, *10*, 566−581.
(20) Diebold, U. Structure and properties of TiO 2 surfaces: a brief review. *Appl. Phys. A: Mater. Sci. Process.* **2003**, *76*, 681−687.
(21) Vandebriel, R. J. The Crystal Structure of Titanium Dioxide Nanoparticles Influences Immune Activity in Vitro and in Vivo. Part. *Fibre Toxicol.* **2018**, *15*, 9.
(22) Gupta, S. M.; Tripathi, M. A review of TiO2 nanoparticles. *Chin. Sci. Bull.* **2011**, *56*, 1639−1657.
(23) Smirnova, N.; Fesenko, T.; Zhukovsky, M.; Goworek, J.; Eremenko, A. Photodegradation of Stearic Acid Adsorbed on Superhydrophilic TiO2 Surface: In Situ FT-IR and LDI Study. *Nanoscale Res. Lett.* **2015**, *10*, 500.
(24) Malik, H.; Barrera, K.; Mohanty, S.; Carlson, K. Enhancing electrochemical properties of TiO2 nanotubes via engineered defect laden crystal structures. *Materials Letters* **2020**, *273*, 127956.
(25) Stoppa, A.; Chiolerio, A. Wearable Electronics and Smart Textiles: A Critical Review. *Sensors* **2014**, *14*, 11957−11992.
(26) Yin, C.; Wang, T.; Che, Z.; Jia, M.; Sun, K. Oblique Impact of Droplets on Microstructured Superhydrophobic Surfaces. *Int. J. Heat Mass Transfer* **2018**, *123*, 693−704.
(27) Reyes-Coronado, D.; Rodríguez-Gattorno, G.; Espinosa-Pesqueira, M. E.; Cab, M. E.; de Coss, C.; Oskam, R.; Oskam, G. Phase-pure TiO2nanoparticles: anatase, brookite and rutile. *Nanotechnology* **2008**, *19*, 145605.
(28) Fischer, K.; Gawel, A.; Prager, A. Low-Temperature Synthesis of Anatase/Rutile/Brookite TiO_2 Nanoparticles on a Polymer Membrane for Photocatalysis. *Catalysts* **2017**, *7*, 209.
(29) Di Paola, A.; Bellardita, M.; Palmisano, L. Brookite, the Least Known TiO2 Photocatalyst. *Catalysts* **2013**, *3*, 36−73.
(30) Hoerr, C. W.; Balston, A. W. The Solubilities of the Normal Saturated Fatty Acids. Ii. *J. Org. Chem.* **1944**, *09*, 329−337.
(31) Deng, J.; Jia, G. Dielectric Constant Prediction of Pure Organic Liquids and Their Mixtures with Water based on Interpretable Machine Learning. *Fluid Phase Equilib.* **2022**, *561*, 113545.
(32) Lee, N. S.; Kang, H.; Ito, E.; Hara, M.; Noh, J. Effects of Solvent on the Structure of Octanethiol Self-Assembled Monolayers on Au(111) at a High Solution Temperature. *Bull. Korean Chem. Soc.* **2010**, *31*, 2137.
(33) Lee, S. Y.; Noh, J.; Ito, E.; Lee, H.; Hara, M. Solvent Effect on Formation of Cysteamine Self-Assembled Monolayers on Au(111). *Jpn. J. Appl. Phys.* **2003**, *42*, 236−241.
(34) Chen, X.; Luais, E.; Darwish, N.; Ciampi, S.; Thordarson, P.; Gooding, J. J. Studies on the Effect of Solvents on Self-Assembled Monolayers Formed from Organophosphonic Acids on Indium Tin Oxide. *Langmuir* **2012**, *28*, 9487−9495.

https://doi.org/10.1021/acsomega.2c06217
ACS Omega 2022, 7, 48184−48191